TECHNISCHE MECHANIK, Band 19, Heft 1, (1999), 19-27
Manuskripteingang: 20. April 1998

Error-Controlled Runge-Kutta Time Integration of a Viscoplastic Hybrid Two-Phase Model

S. Diebels, P. Ellsiepen, W. Ehlers

A hybrid two-phase model consisting of a materially incompressible solid skeleton saturated by a compressible pore-fluid is presented. The material behaviour of the solid phase is assumed to be elastic-viscoplastic, with the viscoplastic part being modelled by a single surface yield condition and a non-associated flow rule. The numerical solution of initial-boundary value problems is based on the finite element method for spatial discretisation, while the time integration of the resulting semi-discrete system of differential-algebraic equations is performed by an embedded error-controlled Runge-Kutta scheme. It is found that, especially in the presence of localisation phenomena, error control is essential to obtain the correct solutions.

1 Introduction

The mechanical behaviour of multi-phase materials is of interest in several branches of engineering, e. g. in geomechanics, soil mechanics, powder metallurgy, and biomechanics. The theoretical access to these fields is by the theory of porous media (TPM), a macroscopic theory of superimposed continua which is based on the theory of mixtures and combined with the concept of volume fractions. In this theory, the properties of the constituents (phases) are averaged over a representative elementary volume (REV) occupied by the whole mixture. Therefore, in the resulting homogenised or "smeared" model, material points of each constituent exist at each geometrical point. The volume fractions are introduced as scalar structural variables which describe the local composition of the mixture. This approach has been discussed in detail by Bowen (1980, 1982), de Boer and Ehlers (1986), Ehlers (1993, 1996), and others. Applications of the TPM in terms of numerical computations based on two-phase models usually deal with a microscopically incompressible solid skeleton which is saturated by an incompressible viscous pore-fluid. Therein, the material behaviour of the skeleton ranges from elastic (Prévost, 1982; Diebels and Ehlers, 1996), elastic-plastic (Ehlers, Diebels, Ellsiepen and Volk, 1997; Ehlers and Volk, 1998) to elastic-viscoplastic (Diebels, Ellsiepen and Ehlers, 1996).

This paper deals with a so-called hybrid model (Ehlers, 1993), i. e. a microscopically incompressible solid skeleton saturated by a compressible pore-fluid. Such a model is able to describe the behaviour of porous media such as dry soils, metallic or polymeric foams and other porous materials which are saturated by a gas. The following section gives a brief outline of the kinematic relations governing the hybrid two-phase model. Section 3 discusses the balance equations, whereas section 4 is assigned to the constitutive equations modelling an elastic-viscoplastic skeleton and a viscous compressible pore-fluid, restricted to the geometrically linear theory. In section 5, the spatial discretisation of the governing equations by the finite element method (FEM) leads to a system of differential-algebraic equations (DAE) in time. Numerical integration of this system is performed by a Runge-Kutta method with embedded error estimator and step size adaption. For details concerning differential-algebraic equations, see e. g. Brenan, Campbell and Petzold (1989), Hairer, Lubich and Roche (1989), Hairer and Wanner (1991).

2 Kinematics

The theory of porous media is based on the assumption of superimposed continua, that is, within a macroscopic theory, the constituents are averaged over the REV and, therefore, each spatial point is occupied by material points of all constituents. Quantities belonging to a constituent (phase) φ^α are characterised by an index α. The local structure of the mixture is represented by scalar variables, the

volume fractions n^α, describing the local ratio of the volume occupied by a phase φ^α (volume element $\mathrm{d}v^\alpha$) and the bulk volume occupied by the whole mixture φ (volume element $\mathrm{d}v$):

$$n^\alpha = \frac{\mathrm{d}v^\alpha}{\mathrm{d}v} \tag{1}$$

In a two-phase mixture ($\alpha \in \{S, F\}$) consisting of a solid skeleton φ^S and a pore-fluid φ^F, the saturation constraint reads $n^S + n^F = 1$. Starting from different reference positions $\mathbf{X}_\alpha$, each constituent follows its own motion

$$\mathbf{x} = \boldsymbol{\chi}_\alpha(\mathbf{X}_\alpha, t) \tag{2}$$

which leads to the velocities $\mathbf{x}'_\alpha = \partial\boldsymbol{\chi}_\alpha(\mathbf{X}_\alpha, t)/\partial t$ and accelerations $\mathbf{x}''_\alpha = \partial^2\boldsymbol{\chi}_\alpha(\mathbf{X}_\alpha, t)/\partial t^2$. The deformation gradient is computed from equation (2) by $\mathbf{F}_\alpha = \partial\boldsymbol{\chi}_\alpha(\mathbf{X}_\alpha, t)/\partial\mathbf{X}_\alpha =: \mathrm{Grad}_\alpha\,\mathbf{x}$. Using a Lagrangean description of the solid phase φ^S, the primary variable is the displacement vector $\mathbf{u}_S$, leading to the velocity $\mathbf{v}_S$:

$$\mathbf{u}_S = \mathbf{x} - \mathbf{X}_S \qquad \mathbf{v}_S = \mathbf{x}'_S = (\mathbf{u}_S)'_S \tag{3}$$

In contrast to the usual Eulerian description, the fluid phase is described relative to the deforming skeleton by the so-called seepage velocity, i. e. the difference velocity between the solid and the fluid motion:

$$\mathbf{w}_F = \mathbf{x}'_F - \mathbf{x}'_S \tag{4}$$

Restricting the presentation to the geometrically linear case, the spatial derivatives $\mathrm{grad}(\cdot) = \partial(\cdot)/\partial\mathbf{x}$ and $\mathrm{Grad}_\alpha(\cdot) = \partial(\cdot)/\partial\mathbf{X}_\alpha$ are approximately equivalent. Therefore, the linear strain tensor reads

$$\boldsymbol{\varepsilon}_S = \frac{1}{2}\big(\mathrm{grad}\,\mathbf{u}_S + \mathrm{grad}^T\,\mathbf{u}_S\big) \tag{5}$$

where the transposition of a second-order tensor is indicated by $(\cdot)^T$, and $\mathrm{grad}^T(\cdot) = (\mathrm{grad}(\cdot))^T$.

3 Balance Equations

The balance equations can be derived based on the framework of a master balance discussed in detail by Ehlers (1996). With the partial density $\rho^\alpha = n^\alpha\rho^{\alpha R}$, the effective density $\rho^{\alpha R}$, and the material time derivative $(\rho^\alpha)'_\alpha = \partial\rho^\alpha/\partial t + \mathrm{grad}\,\rho^\alpha \cdot \mathbf{x}'_\alpha$ following the motion of φ^α, the balance of mass for φ^α reads

$$\big(\rho^\alpha\big)'_\alpha + \rho^\alpha\,\mathrm{div}\,\mathbf{x}'_\alpha = 0 \tag{6}$$

The operator $\mathrm{div}(\cdot)$ is the divergence corresponding to $\mathrm{grad}(\cdot)$. For a microscopically incompressible solid skeleton, the effective density ρ^{SR} is constant, while the partial density ρ^S may vary due to changes in the volume fraction n^S. The solid balance of mass reduces to a volume balance which can be integrated from an initial-value n^S_{0S} leading to

$$n^S = n^S_{0S}\,\det\mathbf{F}_S^{-1} \approx n^S_{0S}\big(1 - \mathrm{div}\,\mathbf{u}_S\big), \tag{7}$$

where the second identity is valid in the framework of the geometrically linear theory. The volume fraction $n^F = 1 - n^S$ of the fluid is obtained from the saturation constraint. Splitting the fluid density into the volume fraction n^F and its effective part ρ^{FR}, substituting the fluid velocity $\mathbf{x}'_F = \mathbf{x}'_S + \mathbf{w}_F$ from equation (4), and applying the identity $(\cdot)'_F = (\cdot)'_S + [\mathrm{grad}(\cdot)]\cdot\mathbf{w}_F$ to $(n^F)'_F$ and $(\rho^{FR})'_F$ in order to formulate the model with the time derivative $(\cdot)'_S$ only, the fluid balance of mass (6) becomes

$$n^F\big(\rho^{FR}\big)'_S + \rho^{FR}\,\mathrm{div}\,\big(\mathbf{u}_S\big)'_S + \mathrm{div}\big(n^F\rho^{FR}\mathbf{w}_F\big) = 0 \tag{8}$$

Neglecting acceleration terms, the balance of (linear) momentum for each constituent φ^α reads

$$\mathbf{0} = \operatorname{div} \mathbf{T}^\alpha + \rho^\alpha \mathbf{b}^\alpha + \hat{\mathbf{p}}^\alpha \tag{9}$$

with the partial Cauchy stress tensors $\mathbf{T}^\alpha$, body forces $\mathbf{b}^\alpha$, and the momentum exchange $\hat{\mathbf{p}}^S = -\hat{\mathbf{p}}^F$ (interaction force). As discussed by Diebels and Ehlers (1996), it is useful to deal with the mixture balance of momentum instead of the solid's balance. The sum of both momentum balances is given by

$$\mathbf{0} = \operatorname{div}(\mathbf{T}^S + \mathbf{T}^F) + (\rho^S + \rho^F)\mathbf{g} \tag{10}$$

where the body forces $\mathbf{b}^\alpha$ are identified with the gravity $\mathbf{g}$.

4 Constitutive Equations

From general thermodynamical considerations (Ehlers, 1993), the stress tensors $\mathbf{T}^\alpha$ and the interaction term $\hat{\mathbf{p}}^F$ have the following structure:

$$\begin{aligned} \mathbf{T}^S &= -n^S p\, \mathbf{I} + \mathbf{T}_E^S \\ \mathbf{T}^F &= -n^F p\, \mathbf{I} + \mathbf{T}_E^F \\ \hat{\mathbf{p}}^F &= p \operatorname{grad} n^F + \hat{\mathbf{p}}_E^F \end{aligned} \tag{11}$$

In case of the hybrid model under consideration, both the extra quantities, index $(\cdot)_E$, and the effective pressure p are determined by constitutive equations as functions of the process variables. Otherwise, i. e. when the pore-fluid is incompressible, the pressure p results from a constraint and depends on the boundary conditions of the problem. Here, the compressible fluid phase φ^F is considered to be a pore-gas, and the pressure is determined by an equation of state (ideal gas equation):

$$p = R\,\Theta\,\rho^{FR} \tag{12}$$

Both the general gas constant R and Kelvin's temperature Θ are assumed to be constant. As usual in hydraulics, the extra fluid stresses are neglected. Fluid friction is modelled by the extra term of the interaction force only:

$$\hat{\mathbf{p}}_E^F = -\frac{(n^F)^2 \gamma^{FR}}{k^F}\, \mathbf{w}_F \tag{13}$$

The Darcy permeability k^F is a macroscopic quantity containing information on the pore size and structure and on the fluid viscosity. In combination with the quasi-static momentum balance of the fluid, this representation of the interaction term leads to the well known Darcy law. The extra stresses of the solid skeleton are determined by an elastic-viscoplastic material law. Therefore, in the framework of a geometrically linear theory, the strain tensor $\boldsymbol{\varepsilon}_S$ is additively decomposed into its elastic and plastic parts

$$\boldsymbol{\varepsilon}_S = \boldsymbol{\varepsilon}_{Se} + \boldsymbol{\varepsilon}_{Sp} \tag{14}$$

The linear extra stress tensor $\boldsymbol{\sigma}_E^S \approx \mathbf{T}_E^S$ depends on the elastic part of the strain only,

$$\boldsymbol{\sigma}_E^S = 2\,\mu^S\, \boldsymbol{\varepsilon}_{Se} + \lambda^S \operatorname{tr} \boldsymbol{\varepsilon}_{Se}\, \mathbf{I} \tag{15}$$

where μ^S and λ^S are the Lamé constants of the Hooke-type elasticity law. Note that λ^S represents a structural compressibility since the skeleton material is microscopically incompressible. Following the basic ideas of Perzyna (1966), the plastic strain is the result of a flow rule

$$\left(\boldsymbol{\varepsilon}_{Sp}\right)'_S = \Lambda \frac{\partial G}{\partial \boldsymbol{\sigma}_E^S} \qquad \Lambda = \frac{1}{\eta} \left\langle \frac{F(\mathrm{I}, \mathrm{II}_D, \mathrm{III}_D)}{\sigma_0} \right\rangle^r \tag{16}$$

where the plastic multiplier Λ is determined by a yield criterion F and the flow direction is derived from a viscoplastic potential G. The viscous parameters are the relaxation time η, the stress normalisation σ_0 and the exponent r. The Föppel symbol (Macauley brackets) is defined by $\langle x \rangle = (x + |x|)/2$. The present formulation is based on the single surface yield criterion proposed by Ehlers (1995),

$$\begin{aligned} F(\mathrm{I}, \mathrm{II}_D, \mathrm{III}_D) &= \sqrt{\mathrm{II}_D \left(1 + \gamma \, \mathrm{III}_D / \mathrm{II}_D^{3/2}\right)^m + \tfrac{1}{2}\alpha \, \mathrm{I}^2 + \delta^2 \, \mathrm{I}^4} + \beta \mathrm{I} + \varepsilon \mathrm{I}^2 - \kappa \\ &\text{with } F(\mathrm{I}, \mathrm{II}_D, \mathrm{III}_D) \begin{cases} < 0 & \text{elastic} \\ \geq 0 & \text{viscoplastic} \end{cases} \end{aligned} \tag{17}$$

In addition, the viscoplastic potential proposed by Diebels, Ellsiepen and Ehlers (1996),

$$G(\mathrm{I}, \mathrm{II}_D) = \sqrt{\mathrm{II}_D + \tfrac{1}{2}\alpha \, \mathrm{I}^2 + \delta \, \mathrm{I}^4} + \beta \mathrm{I} + \varepsilon \, \mathrm{I}^2 + g(\mathrm{I}) \tag{18}$$

is applied. The yield criterion F and the viscoplastic potential G depend on the first invariant I of the extra stress tensor $\boldsymbol{\sigma}_E^S$ and the second and third invariants II_D and III_D of the extra stress deviator $\boldsymbol{\sigma}_E^{SD}$. The material parameters α, β, γ, δ, ε, κ, m, η, σ_0, and r have to be determined from (triaxial) experiments, the function $g(\mathrm{I})$ allows to adjust the course of the dilatation angle ν_p.

5 Numerical Solution

The numerical solution of initial-boundary value problems with the presented hybrid model requires that the governing equations be discretised both in the spatial and in the time domain.

Spatial Discretisation. The spatial discretisation with the finite element method is based on a weak formulation of the governing equations (mixture balance of momentum equation (10) and fluid balance of mass equation (8) together with the ideal gas equation (12) and the Darcy law). The primary variables are $\mathbf{u}_S$ and p. In case of the incompressible two-phase model, this procedure is given in detail by Diebels and Ehlers (1996). Multiplying the equations by test functions $\delta\mathbf{u}_S$ and δp and integrating by parts results in the weak formulation of the hybrid two-phase model:

$$\begin{aligned} &\int_\Omega \operatorname{grad} \delta\mathbf{u}_S \cdot (\boldsymbol{\sigma}_E^S - p\,\mathbf{I}) \, dv = \int_\Omega \delta\mathbf{u}_S \cdot (\rho^S + \rho^F)\,\mathbf{g} \, dv + \int_{\Gamma_t} \delta\mathbf{u}_S \cdot \bar{\mathbf{t}} \, da \\ &\frac{1}{R\Theta} \int_\Omega \delta p \, [n^F p'_S + p \operatorname{div} (\mathbf{u}_S)'_S] \, dv + \frac{1}{R\Theta} \int_\Omega \operatorname{grad} \delta p \cdot \frac{k^F}{g} \operatorname{grad} p \, dv = \\ &\qquad = \frac{1}{R\Theta} \int_\Omega \operatorname{grad} \delta p \cdot \frac{k^F}{g} \frac{p}{R\Theta} \mathbf{g} \, dv - \int_{\Gamma_q} \delta p \, \bar{q} \, da \end{aligned} \tag{19}$$

Therein, $g = |\mathbf{g}|$ is the acceleration due to gravity, $\bar{\mathbf{t}} = (\boldsymbol{\sigma}_E^S - p\,\mathbf{I})\,\mathbf{n}$ is the force vector acting on the Neumann boundary Γ_t of the mixture and $\bar{q} = n^F \rho^{FR} \mathbf{w}_F \cdot \mathbf{n}$ is the (outward) fluid mass flux

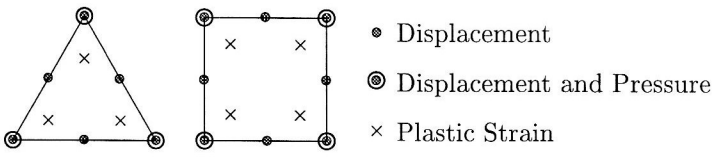

Figure 1. Discretisation with Triangles or Quadrilaterals

through the Neumann boundary Γ_q. As usual, the test functions vanish on Dirichlet boundaries with prescribed displacement or pressure. Within the finite element discretisation, the evolution equation (16)

for the plastic strain ε_{Sp} (internal variable) is computed only at the integration points of the numerical quadrature in the sense of a collocation method. For the displacement $\mathbf{u}_S$, quadratic shape functions are used, while the pressure p is approximated by linear shape functions. In the case of triangles, this type of approximation is known as the Taylor-Hood element, cf. Figure 1. The set of equations resulting from the FEM semi-discretisation is still continuous in the time variable.

Time Integration. For a mesh with N_u nodes and N_q integration points, the FEM degrees of freedom are collected in a vector $\boldsymbol{u}$ and the internal variables in a vector $\boldsymbol{q}$:

$$\begin{aligned} \boldsymbol{u} &= ((\mathbf{u}_S^1, p^1), \dots, (\mathbf{u}_S^{N_u}, p^{N_u}))^T \\ \boldsymbol{q} &= (\boldsymbol{\varepsilon}_{Sp}^1, \dots, \boldsymbol{\varepsilon}_{Sp}^{N_q})^T \end{aligned} \tag{20}$$

With the abbreviation $(\cdot)' = (\cdot)'_S$ and the vector of unknowns $\boldsymbol{y} := (\boldsymbol{u}^T, \boldsymbol{q}^T)^T$, the semi-discrete initial-value problem in time with $t \geq t_0$ can be formulated as follows (Ehlers and Ellsiepen, 1996, 1997):

$$\boldsymbol{F}(t, \boldsymbol{y}, \boldsymbol{y}') \equiv \begin{bmatrix} \boldsymbol{F}_1(t, \boldsymbol{u}, \boldsymbol{u}', \boldsymbol{q}) \\ \boldsymbol{F}_2(t, \boldsymbol{q}, \boldsymbol{q}', \boldsymbol{u}) \end{bmatrix} \equiv \begin{bmatrix} \boldsymbol{M}\,\boldsymbol{u}' + \boldsymbol{k}(\boldsymbol{u}, \boldsymbol{q}) - \boldsymbol{f} \\ \boldsymbol{q}' - \boldsymbol{g}(\boldsymbol{q}, \boldsymbol{u}) \end{bmatrix} \stackrel{!}{=} \mathbf{0} \qquad \boldsymbol{y}(t_0) = \boldsymbol{y}_0 \tag{21}$$

The first equation $\boldsymbol{F}_1$ represents the field equations with a generalised mass matrix $\boldsymbol{M}$, a generalised stiffness vector $\boldsymbol{k}$, and generalised external forces $\boldsymbol{f}$ (FEM degrees of freedom, global). The second equation $\boldsymbol{F}_2$ represents the evolution equations of the plasticity model which are evaluated at the integration points of the finite elements (internal variables, local). Due to the fact that the acceleration terms in the mixture balance of momentum have been neglected (quasi-static model), the matrix $\boldsymbol{M}$ does not possess the full rank. This makes equation (21) a system of differential-algebraic equations (DAE) which can be shown to be of differential index one. Suitable time integration methods for index one DAEs have to fulfil certain stability properties. To name only a few, A-stability is a must as a DAE can be thought of as an infinitely stiff system of ODEs. Furthermore, L-stability is a desirable property for equations that include some physical damping like the presented hybrid two-phase model. In the last twenty years, many other stability concepts have been developed, cf. e. g. Hairer and Wanner (1991).

In what follows, only one-step methods are considered as they provide a suitable means to integrate FEM systems including internal variables (plasticity) at moderate storage and computational costs. Implicit Runge-Kutta methods (IRK) constitute the most prominent class of one-step methods, allowing for flexible construction of methods with various properties, e. g. stability, high order, reusability of linearisation matrices, and embedded error estimations. For details on the convergence of IRK methods applied to DAEs, see Hairer, Lubich and Roche (1989), Brenan, Campbell and Petzold (1989). For large systems

$$\begin{array}{c|ccc} c_1 & a_{11} & & \\ \vdots & \vdots & \ddots & \\ c_s & a_{s1} & \cdots & a_{ss} \\ \hline & b_1 & \cdots & b_s \\ & \hat{b}_1 & \cdots & \hat{b}_s \end{array}$$

Figure 2. Butcher Array for DIRK Methods

as arise in FEM computations, diagonally implicit Runge-Kutta methods (DIRK) are advantageous as they allow the stage solutions to be calculated one after the other, thus reducing the number of unknowns in a single non-linear system solve. For systems with only mild non-linearities, singly diagonally implicit Runge-Kutta methods (SDIRK) additionally allow a once computed and factorised matrix to be reused which, in some cases (Ehlers and Ellsiepen, 1996), can drastically reduce the overall solution time. The coefficients of a general s-stage DIRK method are summarised in the Butcher array shown in Figure 2. The c_i are the quadrature points (stage positions), and the a_{ij} and b_i are the internal and

external weights, respectively. The additional external weights $\hat{b}_i$ provide an embedded method of order $\hat{p} < p$, where p is the order of the native method. Stiffly accurate methods, i. e. $a_{si} = b_i$, are preferred when integrating DAEs as this property guarantees that the algebraic constraints are fulfilled at the new time step. Moreover, consistent initial values are a neccesary assumption, that is, the equation $\boldsymbol{F}(t_0, \boldsymbol{y}_0, \boldsymbol{y}_0') = \boldsymbol{0}$ must have a solution $\boldsymbol{y}_0'$. With a given time step h_n at time t_n, stage derivatives $\boldsymbol{Y}_i'$, stage solutions $\boldsymbol{Y}_i = \boldsymbol{y}_n + h_n \sum_{j=1}^{i} a_{ij} \boldsymbol{Y}_j'$, stage increments $\boldsymbol{z}_i = \boldsymbol{Y}_i - \boldsymbol{y}_n$, and accumulated stage derivatives $\boldsymbol{s}_i = h_n \sum_{j=1}^{i-1} a_{ij} \boldsymbol{Y}_j'$, the main computational effort of the DIRK method is in the solution of the following s non-linear systems for the stage increments $\boldsymbol{z}_i$:

$$\boldsymbol{F}\big(t_n + c_i h_n,\ \boldsymbol{y}_n + \boldsymbol{z}_i,\ \tfrac{1}{h_n a_{ii}}[\boldsymbol{z}_i - \boldsymbol{s}_i]\big) = \boldsymbol{0} \qquad i = 1 \ldots s \tag{22}$$

During the solution of the non-linear systems, the quantities $\boldsymbol{Y}_i'$ have to be stored. Then, the two solutions of order p and $\hat{p}$, respectively, at time $t_{n+1} = t_n + h_n$ may be calculated:

$$\boldsymbol{y}_{n+1} = \boldsymbol{y}_n + h_n \sum_{j=1}^{s} b_i \boldsymbol{Y}_i' \qquad \hat{\boldsymbol{y}}_{n+1} = \boldsymbol{y}_n + h_n \sum_{j=1}^{s} \hat{b}_i \boldsymbol{Y}_i' \tag{23}$$

Clearly, for stiffly accurate methods, the new solution coincides with the solution of the last stage, $\boldsymbol{y}_{n+1} = \boldsymbol{Y}_s = \boldsymbol{y}_n + \boldsymbol{z}_s$, and is not recalculated. An embedded error estimation is given by the difference of the two solutions of orders p and $\hat{p} < p$, respectively:

$$ERR \approx \|\boldsymbol{y}_{n+1} - \hat{\boldsymbol{y}}_{n+1}\| = \|h_n \sum_{j=1}^{s} (b_i - \hat{b}_i) \boldsymbol{Y}_i'\| \tag{24}$$

Note that this error estimation is "cheap" in the sense that it does not require an additional non-linear system solution but only a weighted sum of the already computed quantities $\boldsymbol{Y}_i'$. This makes Runge-Kutta methods with embedded error estimators well suited for large systems of equations.

In the case of the hybrid two-phase model, the non-linear systems (22) read

$$\begin{bmatrix} \boldsymbol{r}_i^1(\boldsymbol{z}_i^1, \boldsymbol{z}_i^2) \\ \boldsymbol{r}_i^2(\boldsymbol{z}_i^2, \boldsymbol{z}_i^1) \end{bmatrix} \equiv \begin{bmatrix} \frac{1}{h_n a_{ii}} \boldsymbol{M}(\boldsymbol{z}_i^1 - \boldsymbol{s}_i^1) + \boldsymbol{k}(\boldsymbol{u}_n + \boldsymbol{z}_i^1,\ \boldsymbol{q}_n + \boldsymbol{z}_i^2) - \boldsymbol{f} \\ \frac{1}{h_n a_{ii}} \quad (\boldsymbol{z}_i^2 - \boldsymbol{s}_i^2) + \boldsymbol{g}(\boldsymbol{q}_n + \boldsymbol{z}_i^2,\ \boldsymbol{u}_n + \boldsymbol{z}_i^1) \end{bmatrix} \stackrel{!}{=} \begin{bmatrix} \boldsymbol{0} \\ \boldsymbol{0} \end{bmatrix} \tag{25}$$

where $\boldsymbol{z}_i^1$ and $\boldsymbol{z}_i^2$ are the stage increments for the FEM nodal variables $\boldsymbol{u}$ and the internal variables $\boldsymbol{q}$, respectively. The special structure of equation (25) is exploited during the solution process, that is, the non-linear systems are solved by a generalised Block-Gauss-Seidel-Newton iteration. In this context, the evolution equations of the plasticity model are solved by a local Newton iteration with fixed increments $\boldsymbol{z}_i^1$ of the global variables, i. e. $\boldsymbol{r}_i^2(\boldsymbol{z}_i^2; \boldsymbol{z}_i^1) = \boldsymbol{0}$, resulting in local increments $\boldsymbol{z}_i^2(\boldsymbol{z}_i^1)$ depending on the fixed global increments. This corresponds to a local evaluation of the constitutive equations in each finite element. The second step of the procedure is the solution of the global sparse linear FEM system $\boldsymbol{J}_i\, \Delta \boldsymbol{z}_i^1 = \boldsymbol{r}_i^1$, taking into account the local algorithm during the linearisation to yield a global Jacobian matrix

$$\boldsymbol{J}_i = \frac{\mathrm{d}\boldsymbol{r}_i^1(\boldsymbol{z}_i^1, \boldsymbol{z}_i^2(\boldsymbol{z}_i^1))}{\mathrm{d}\boldsymbol{z}_i^1} = \frac{\partial \boldsymbol{r}_i^1}{\partial \boldsymbol{z}_i^1} + \frac{\partial \boldsymbol{r}_i^1}{\partial \boldsymbol{z}_i^2} \frac{\mathrm{d}\boldsymbol{z}_i^2}{\mathrm{d}\boldsymbol{z}_i^1} \tag{26}$$

Therein, the first term on the right hand side is the generalised stiffness matrix from the elastic material law (and the linearisation of the Darcy law), while the second term results from the linearisation of the discrete plastic evolution equations. In the literature, this procedure is known as the "algorithmicly consistent linearisation". In case of the implicit Euler integration scheme – which is in fact a special

one-stage SDIRK scheme with all coefficients equal to one – the well known elastic-predictor – plastic-corrector scheme is obtained, cf. e. g. Hartmann, Lührs and Haupt (1997). After the solution of the linear FEM system, the stage increments of the global FEM variables are updated according to Newton's method, $\boldsymbol{z}_i^1 := \boldsymbol{z}_i^1 - \Delta\boldsymbol{z}_i^1$, and the whole procedure is repeated until a suitable convergence criterion is met, e. g. $\|\boldsymbol{r}_i^1\| < TOL_r$ and/or $\|\Delta\boldsymbol{z}_i^1\| < TOL_z$.

Due to the different nature of the quantities $\boldsymbol{u}$ (FEM degrees of freedom in the L_2 sense) and $\boldsymbol{q}$ (collocation variables), the error estimation equation (24) is used to define two tolerance weighted error measures e_u and e_q in a weighted 2-norm and maximum norm, respectively (Ehlers and Ellsiepen, 1997). A time step is accepted if both error measures are less or equal to one, and rejected otherwise. In both cases a new step size is predicted from the error measures and the order $\hat{p}$ of the embedded method:

$$h_{\text{new}} := h_n \cdot \left(\frac{1}{\max\{e_u, e_q\}} \right)^{\frac{1}{\hat{p}+1}} \tag{27}$$

6 Example

A simulation of a biaxial compression test is used as an example. From biaxial experiments it is known that, when a critical load is reached, the plastic strain localises in narrow bands (shear bands). In general, the location and orientation of shear bands are not known. To overcome this difficulty in the numerical simulation, the stiffness of one element is reduced to initiate shear banding as indicated in Figure 3. The lower boundary of the specimen is fixed while at the upper boundary the displacement u_2 is given as a function of time. The horizontal stress t_1 is applied and then kept constant.

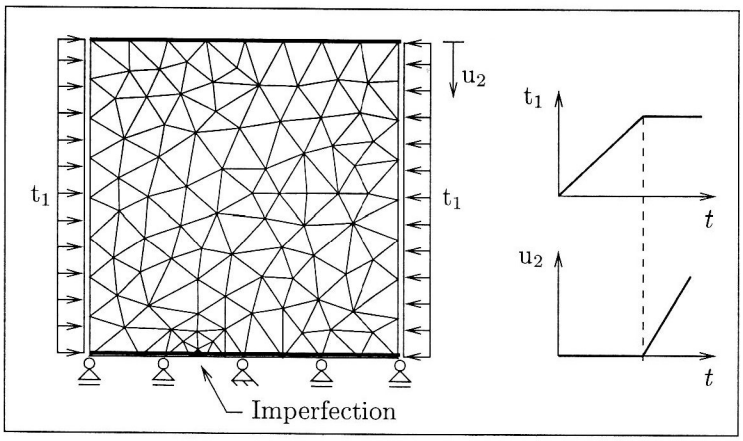

Figure 3: Mesh and Boundary Conditions for the Biaxial Test

Figure 4 shows the results obtained by the implicit Euler scheme (left) and by SDIRK 3(2) (Cash, 1979) of third order with embedded error estimator of second order (right). The step size of the implicit Euler scheme is controlled by the number of Newton iterations, i. e. by the non-linearity of the problem, while in the Runge-Kutta scheme, the embedded error estimator is used for automatic step size control. Due to the imperfection on the lower boundary the shear band should start at the weakened element. Therefore, the Runge-Kutta scheme predicts a physically meaningful result while the solution of the implicit Euler scheme is unphysical. The reason is that the non-linearity-control used with the implicit Euler scheme does not recognise when plastic yielding starts. Therefore, the time of first yielding is not predicted correctly and, as a consequence, the shear band starts from a wrong position. In contrast, the error-controlled Runge-Kutta scheme automatically reduces the step size when the first plastic yielding occurs, and again increases the step size once the shear band is established. The solution depicted in the right figure may also be achieved using the implicit Euler scheme when the maximum step size is kept small enough. However, the computational cost is then much higher than that of the error-controlled SDIRK 3(2) – in the present case about a factor of four.

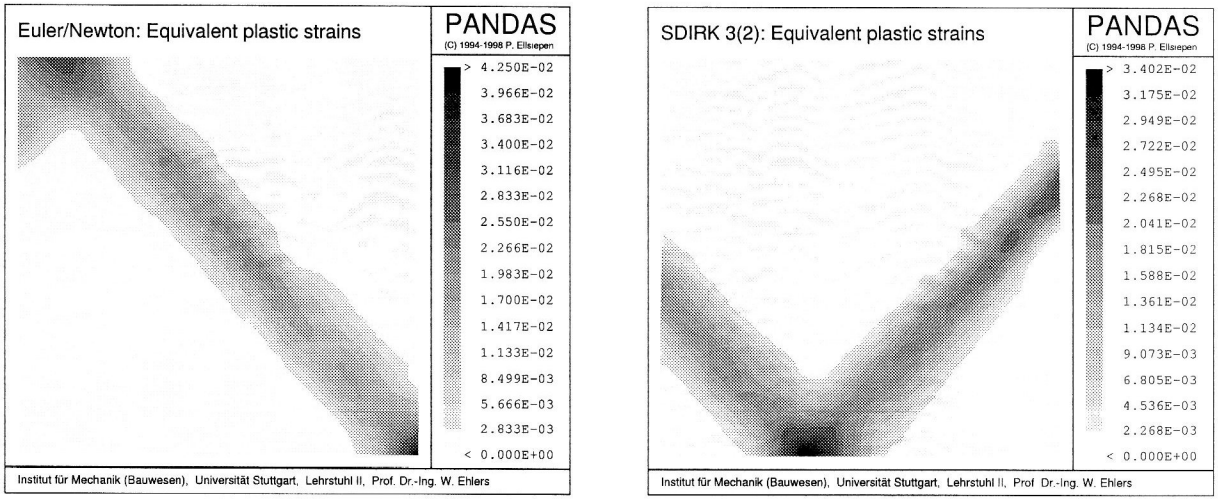

Figure 4. Equivalent Plastic Strains. Left: Implicit Euler, right: SDIRK 3(2)

In general, the correct solution as well as the required step sizes are not known in advance. Therefore, error-controlled schemes, e. g. the SDIRK 3(2) applied here, are neccessary for reliable and efficient numerical time integration of complex initial boundary-value problems that arise in technical applications.

Literature

1. de Boer, R.; Ehlers, W.: Theorie der Mehrkomponentenkontinua mit Anwendung auf bodenmechanische Probleme. Forschungsberichte aus dem Fachbereich Bauwesen, Heft 40, Universität-GH-Essen, (1986).
2. Bowen, R. M.: Incompressible porous media models by use of the theory of mixtures. Int. J. Engng. Sci., 18, (1980), 1129 – 1148.
3. Bowen, R. M.: Compressible porous media models by use of the theory of mixtures. Int. J. Engng. Sci., 20, (1982), 697 – 735.
4. Brenan, K. E.; Campbell, S. L.; Petzold, L. R.: Numerical Solution of Initial-Value Problems in Differential-Algebraic Equations. North-Holland, New York, (1989).
5. Cash, J. R.: Diagonally implicit Runge-Kutta formulæ with error estimates. J. Inst. Maths Applics., 24, (1979), 293 – 301.
6. Diebels, S., Ehlers, W.: Dynamic analysis of a fully saturated porous medium accounting for geometrical and material non-linearities. Int. J. Num. Meth. Engng., 39, (1996), 81 – 97.
7. Diebels, S.; Ellsiepen, P.; Ehlers, W.: A Two-Phase Model for Viscoplastic Geomaterials. Bericht 96-II-6, Institut für Mechanik (Bauwesen), Universität Stuttgart, (1996).
8. Ehlers, W.: Constitutive equations for granular materials in geomechanical context. In K. Hutter (ed.): Continuum Mechanics in Environmental Sciences and Geophysics. CISM Courses and Lectures No. 337, Springer-Verlag, Wien, (1993), 313 – 402.
9. Ehlers, W.: Compressible, incompressible and hybrid two-phase models in porous media theories. In Y. C. Angel (ed.): Anisotropy and Inhomogeneity in Elasticity and Plasticity. AMD-Vol. 158, ASME, New York, (1993), 25 – 38.
10. Ehlers, W.: A single-surface yield function for geomaterials. Arch. Appl. Mech., 65, (1995), 246 – 259.
11. Ehlers, W.: Grundlegende Konzepte in der Theorie Poröser Medien. Technische Mechanik, 16, (1996), 63 – 76.
12. Ehlers, W.; Diebels, S.; Ellsiepen, P.; Volk, W.: Localization phenomena in liquid-saturated soils. In: Proceedings of NAFEMS World Congress 1997, Stuttgart, (1997), 287 – 298.
13. Ehlers, W.; Ellsiepen, P.: Zeitschrittgesteuerte Verfahren bei stark gekoppelten Festkörper-Fluid-Problemen. ZAMM, 77, (1997), S 81 – S 82.

14. Ehlers, W.; Ellsiepen, P.: Adaptive Zeitintegrations-Verfahren für ein elastisch-viskoplastisches Zweiphasenmodell. Bericht 97-II-3, Institut für Mechanik (Bauwesen), Universität Stuttgart, submitted to ZAMM, (1997).
15. Ehlers, W.; Volk, W.: On theoretical and numerical methods in the theory of porous media based on polar and non-polar solid materials. Int. J. Solids Structures, (1998), accepted for publication.
16. Hairer, E.; Lubich, C.; Roche, M.: The Numerical Solution of Differential-Algebraic Equations by Runge-Kutta Methods. Lecture Notes in Mathematics, Springer-Verlag, Berlin, Heidelberg, (1989).
17. Hairer, E.; Wanner, G.: Solving Ordinary Differential Equations II – Stiff and Differential-Algebraic Problems. Springer-Verlag, Berlin, Heidelberg, (1991).
18. Hartmann, S; Lührs, G.; Haupt, P.: An efficient stress algorithm with applications in viscoplasticity and plasticity. Int. J. Num. Meth. Engng., 40, (1997), 991 – 1013.
19. Perzyna, P.: Fundamental problems in viscoplasticity. Adv. Appl. Mech., 9, (1966), 243 – 377.
20. Prévost, J. H.: Nonlinear transient phenomena in saturated porous media. Comp. Methods Appl. Mech. Eng., 30, (1982), 3–18.

Addresses: Dr.-Ing. Stefan Diebels, Dipl.-Math. Peter Ellsiepen, and Prof. Dr.-Ing. Wolfgang Ehlers, Institut für Mechanik (Bauwesen), Lehrstuhl II, Universität Stuttgart, D-70550 Stuttgart, Germany.